

A Methyl 4-Oxo-4-phenylbut-2-enoate with in Vivo Activity against MRSA That Inhibits MenB in the Bacterial Menaquinone Biosynthesis Pathway

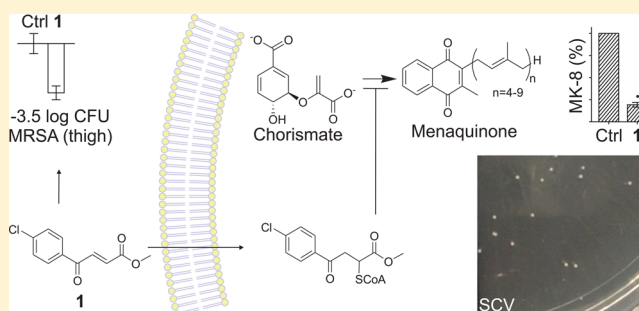
Joe S. Matarlo,^{†,||} Yang Lu,^{†,||} Fereidoon Daryaee,[†] Taraneh Daryaee,[†] Bela Ruzsicska,[†] Stephen G. Walker,[‡] and Peter J. Tonge^{*,†}

[†]Institute of Chemical Biology & Drug Discovery, Department of Chemistry, and [‡]Department of Oral Biology and Pathology, Stony Brook University, Stony Brook, New York 11794-3400, United States

Supporting Information

ABSTRACT: 4-Oxo-4-phenylbut-2-enoates inhibit MenB, the 1,4-dihydroxyl-2-naphthoyl-CoA synthase in the bacterial menaquinone (MK) biosynthesis pathway, through the formation of an adduct with coenzyme A (CoA). Here, we show that the corresponding methyl butenoates have minimum inhibitory concentration (MIC) values as low as 0.35–0.75 $\mu\text{g}/\text{mL}$ against drug-sensitive and -resistant strains of *Staphylococcus aureus*. Mode of action studies on the most potent compound, methyl 4-(4-chlorophenyl)-4-oxobut-2-enoate (**1**), reveal that **1** is converted into the corresponding CoA adduct in *S. aureus* cells and that this adduct binds to the *S. aureus* MenB (*saMenB*) with a K_d value of 2 μM . The antibacterial spectrum of **1** is limited to bacteria that utilize MK for respiration, and the activity of **1** can be complemented with exogenous MK or menadione. Finally, treatment of methicillin-resistant *S. aureus* (MRSA) with **1** results in the small colony variant phenotype, and thus **1** phenocopies knockout of the *menB* gene. Taken together, the data indicate that the antibacterial activity of **1** results from a specific effect on MK biosynthesis. We also evaluated the in vivo efficacy of **1** using two mouse models of MRSA infection. Notably, compound **1** increased survival in a systemic infection model and resulted in a dose-dependent decrease in bacterial load in a thigh infection model, validating MenB as a target for the development of new anti-MRSA candidates.

KEYWORDS: menaquinone biosynthesis, *Staphylococcus aureus*, MenB, electrophilic antibacterial compound, DHNA, menadione



There is an urgent need to identify new drug targets to combat the rising threat of antibiotic-resistant bacteria including methicillin-resistant *Staphylococcus aureus* (MRSA), which the Centers for Disease Control and Prevention (CDC) ranks as one of the top 10 “serious threats” in the United States.^{1–4} *S. aureus* infection is the leading cause of nosocomial dermatitis, folliculitis, osteomyelitis, endocarditis, and bacteremia worldwide,^{5–9} and the cost of treating these infections is currently \$20 billion per year.^{10,11} Vancomycin is the drug of last resort for treating MRSA infection, but the advent of vancomycin-resistant strains of *S. aureus* in clinical settings^{12,13} mitigates the development of new chemotherapeutics to treat these highly dangerous strains.

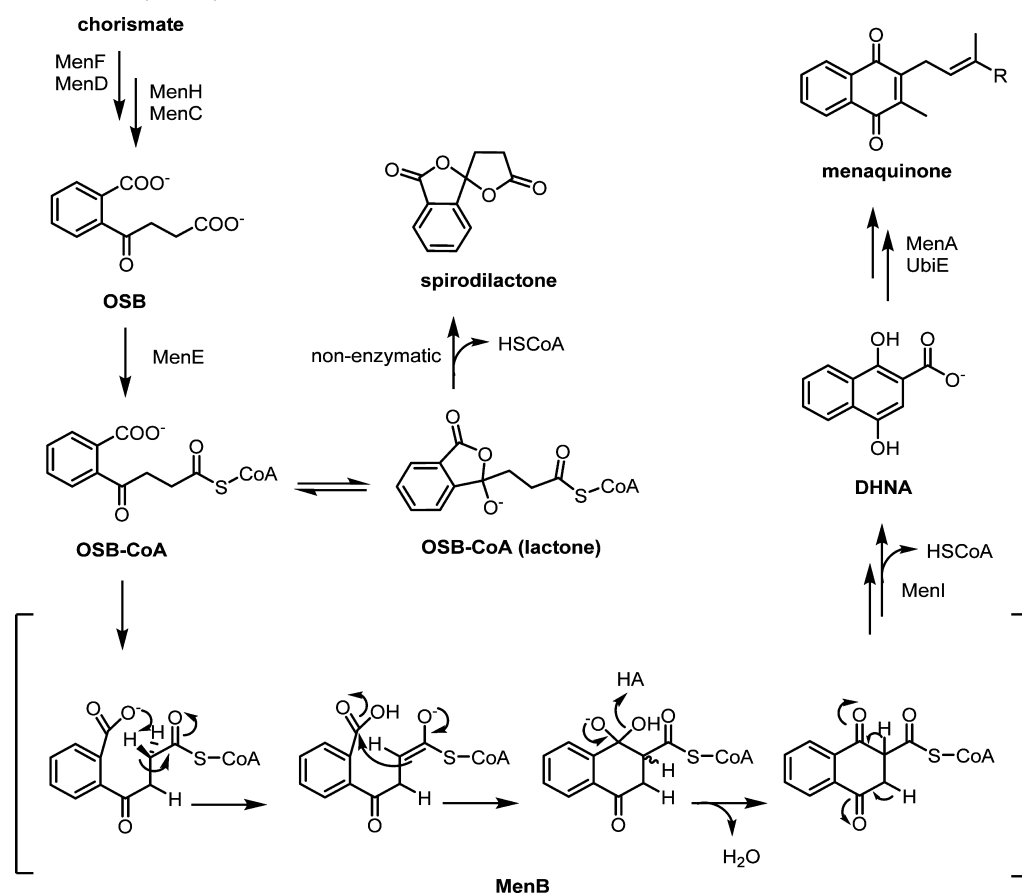
One major hurdle to treating *S. aureus* infection is the ability of this organism to persist in a slow growth small colony variant (SCV) phenotype. Although many bacteria are known to form SCVs as a natural survival mechanism,^{14–17} *S. aureus* SCVs hamper rapid clinical diagnosis and complicate routine laboratory tests, often leading to misidentification and ultimately misdiagnosis. Furthermore, due to the slow growth characteristics of *S. aureus* SCVs, clinical studies have shown that they are

highly drug resistant, less prone to eliciting strong immune responses, and a source of persistent infection.^{18–22} Thus, it is important to treat *S. aureus* infection with therapeutic agents at drug concentrations at which SCVs are not induced²³ and to develop antimicrobial agents that act specifically on SCVs. The SCV phenotype can arise from genetic and metabolic defects,^{24–26} environmental pressure,^{27,28} and metabolite auxotrophism.^{25,29,30} Three well-defined SCV auxotrophisms have been identified in which wild-type growth can be restored by supplementation with thymidine,³¹ CO₂,^{27,32} and molecules that complement deficiencies in electron transport.^{33–35} Typically, for electron-transport-deficient SCVs, the wild-type phenotype can be restored by supplementation with menaquinone (MK, vitamin K2) or menadione (MD, vitamin K3).^{34,36} In some cases, this auxotrophism has been directly linked to mutations in enzymes that constitute the MK biosynthesis pathway.^{34,36,37}

Received: February 7, 2016

Published: March 7, 2016

Scheme 1. Classical Pathway for Menaquinone (MK) Biosynthesis in Organisms such as *S. aureus*, *E. coli*, and *M. tuberculosis* Showing the Reaction Catalyzed by MenB^a



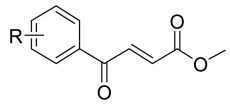
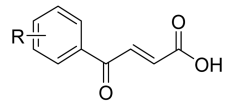
^aOriginal details of this pathway are summarized in Meganathan.⁷⁰ More recently, it has been shown that MenH converts SEPHCHC to SHCHC (SHCHC synthase).⁷¹ In addition, a dedicated DHNA-CoA thioesterase (MenI) has been identified in phyloquinone (vitamin K1) biosynthesis,⁷² and a bacterial homologue of this enzyme has potentially been identified in *E. coli*.⁷³ The classical pathway is distinct from the pathway that proceeds via futasolose in *Streptomyces*.⁷⁴ Also shown is the nonenzymatic decomposition of OSB-CoA to spirodilactone.

S. aureus and other Gram-positive bacteria utilize MK during oxidative and fermentative respiration as an electron carrier in the electron transport chain (Figure S1).^{38,39} The classical de novo MK biosynthesis pathway consists of at least nine distinct enzymes (Scheme 1) and is absent in humans, making MK biosynthesis an attractive therapeutic target. Enzymes in this pathway have been implicated in the survival and virulence of many human pathogens, and several classes of inhibitors have been developed to interrogate the pathway as a prelude to novel antibacterial discovery.^{40–44} In our own studies, we have undertaken detailed characterization and inhibition studies of several enzymes in the pathway including MenB, the 1,4-dihydroxynaphthol-CoA synthase. Mutations in MenB have been shown to correlate with *S. aureus* strains that are auxotrophic for menadione,³⁶ and genetic approaches have demonstrated that MenB is essential for the growth of *M. tuberculosis*.⁴⁵

MenB is the sixth enzyme in the MK pathway and catalyzes an intramolecular Claisen condensation (Dieckmann) reaction leading to the formation of 1,4-dihydroxynaphthoyl-CoA (DHNA-CoA).⁴⁶ We previously conducted a high-throughput screen on MenB from *Mycobacterium tuberculosis* (*mtMenB*) and identified several classes of *mtMenB* inhibitors including the 4-oxo-4-phenyl-2-aminobutanoates.⁴¹ We subsequently demonstrated that elimination of the 2-amino substituent occurs in

aqueous solution to generate the corresponding butenoate, which reacts with CoA to form an adduct that inhibits MenB (Figure S2).^{46–49} We also reported that whereas the butenoate CoA adducts were potent *mtMenB* inhibitors in vitro (K_i 50 nM), the corresponding butenoic acids were poor bacterial growth inhibitors (minimum inhibitory concentration (MIC) = 25 $\mu\text{g}/\text{mL}$ against H37Rv). In contrast, the corresponding methyl butenoates were found to have promising MICs (MIC < 1 $\mu\text{g}/\text{mL}$ H37Rv), suggesting that protection of the carboxylate aids cell penetration. We now extend these studies to probe their mode of action in *S. aureus*. We first demonstrate that the methyl 4-oxo-4-phenyl-2-butenates are active against both drug-sensitive *S. aureus* (MSSA) and MRSA in vitro and that their spectrum of activity extends to other bacteria that synthesize MK. We subsequently show that treatment of MRSA cells with the most potent methyl butenoate (**1**) leads to formation of the corresponding CoA adduct and results in the SCV growth phenotype, thus phenocopying knockout of the *menB* gene. In addition, we demonstrate that compound **1** reduces levels of both MK and DHNA, a downstream product of MenB, and that the antibacterial activity of **1** can be rescued by supplementation with exogenous MK, supporting the proposed mode of action. Finally, we find that the most potent methyl ester conjugate is active against MRSA in mouse models, where it can prolong survival time and reduce bacterial load.

Table 1. In Vitro Antibacterial Activity of the 4-Oxo-4-phenyl-2-butenic Acids and Methyl Esters against *S. aureus*

Compound	Structure	R	MIC ($\mu\text{g/mL}$) ^a	
			MSSA ^b	MRSA ^b
1		4-Cl	0.35	0.75
2		4-F	8	12
3		4-Br	8	16
4		4-NO ₂	4	4
5		2,4-Cl	1	2
6		4-Cl	> 60	> 60
Oxacillin		0.1	>128	
Vancomycin		2	4	

^aModal value of experimental triplicates. ^bMSSA, methicillin-sensitive *S. aureus*; MRSA, methicillin-resistant *S. aureus*. Oxacillin and vancomycin were used as controls.

Table 2. Antibacterial Spectrum of **1** in Menaquinone (MK) and Ubiquinone (Q) Producing Human Pathogens^a

pathogen	electron carrier ^b	MIC aerobic ($\mu\text{g/mL}$)	MIC capnophilic ^c ($\mu\text{g/mL}$)	MIC anaerobic ^c ($\mu\text{g/mL}$)	+ MK-4 ^d
MRSA	MK	0.75	0.37	0.37	>60
<i>B. subtilis</i>	MK	8	4	2	>60
<i>E. faecium</i>	MK	4	2.5	1.25	31.5
<i>E. coli</i>	Q/MK	>60	15.5	15.5	>60
<i>P. aeruginosa</i> ^e	Q	>60	>60	>60	
<i>H. influenzae</i>	dMK/MK		0.25		>60
<i>K. pneumoniae</i> ^e	Q/MK	>60	> 60	62.5	>60
<i>P. mirabilis</i> ^e	Q/MK	>60	12.5	12.5	31.5
<i>M. smegmatis</i>	MK	0.5	0.25		>60
<i>M. tuberculosis</i> ^f	MK	0.64	1.5		

^aMIC values are the modal values of technical and experimental triplicates. ^bQ, ubiquinone; MK, menaquinone; dMK, demethylMK (Scheme 1). ^cMICs determined under capnophilic (candle) or anaerobic (GasPak) conditions by culturing bacteria in a candle jar (see Materials and Methods for complete protocol). ^dMIC value obtained following supplementation with 10 μM commercially available menaquinone-4 (MK-4). ^eActivity of **1** against *P. aeruginosa*, *K. pneumoniae*, and *P. mirabilis* was determined in the presence or absence (no change in MIC) of ¹/₂MIC polymyxin B under aerobic conditions. ^fMIC values reported in Li et al.⁴¹ under aerobic and low oxygen (LORA) conditions.

RESULTS AND DISCUSSION

Methyl 4-Oxo-4-(4-chlorophenyl)-2-butenate (1) Has Potent Activity against *S. aureus*. Previously, we identified a series of 4-oxo-4-phenyl-2-butenate inhibitors of the MenB from *M. tuberculosis* and demonstrated that the corresponding methyl esters had potent antibacterial activity against replicating and nonreplicating *M. tuberculosis* (0.6–1.5 $\mu\text{g/mL}$).⁴¹ To explore the activity and mode of action of these compounds in *S. aureus*, we first evaluated the whole cell antibacterial activity of several methyl butenoates against methicillin-sensitive and -resistant *S. aureus* (MSSA and MRSA, respectively). The minimum inhibitory concentrations (MIC) are summarized in Table 1, where it can be seen that the 4-chloro analogue **1** has the most promising antibacterial activity with MIC values of 0.35 and 0.75 $\mu\text{g/mL}$ against MSSA and MRSA, respectively. We subsequently focused our efforts on interrogating the mode of action of **1** in *S. aureus*.

1 Is a Specific Inhibitor for MK-Utilizing Bacteria. Bacteria generally utilize structural analogues of either ubiquinone (Q) or MK as the lipid-soluble redox active electron carrier in the electron transport chain. To explore the spectrum of antibacterial activity, we thus selected bacteria that use either Q or MK for respiration. The Gram-positive bacteria *Bacillus subtilis* and *Enterococcus faecium*, as well as *Mycobacterium smegmatis* and the Gram-negative bacterium *Haemophilus influenzae*, use MK when grown either aerobically or anaerobically. Conversely, *Pseudomonas aeruginosa* uses Q under all growth conditions, whereas the Gram-negative bacteria *Escherichia coli*, *Klebsiella pneumoniae*, and *Proteus mirabilis* use Q under aerobic growth conditions but switch to MK when grown anaerobically (Table 2). Antibacterial assays revealed that **1** was only active under growth conditions where MK was the primary electron carrier. Thus, **1** was active against *B. subtilis*, *E. faecium*, and *M. smegmatis*, under aerobic, capnophilic, and anaerobic growth conditions, consistent with our previous work in which **1** demonstrated MIC values of 0.64 and 1.5 $\mu\text{g/mL}$ against

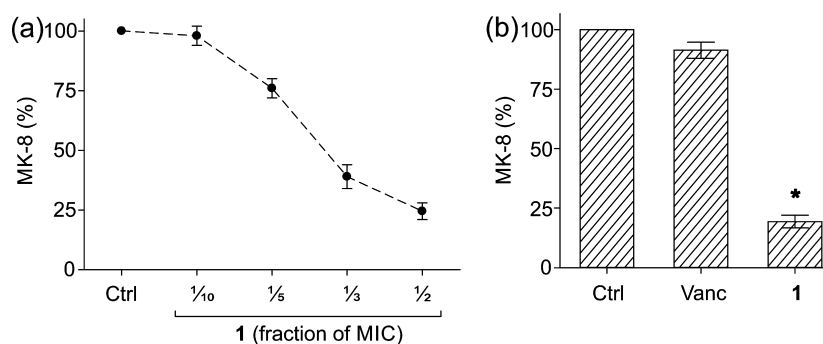
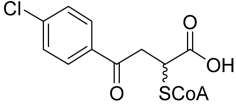
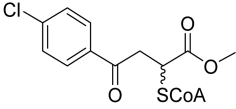


Figure 1. Menaquinone-8 (MK-8) quantification in MRSA cells treated with 1: (a) change in MK-8 levels determined in MRSA treated with sub-MICs ($1/10$, $1/5$, $1/3$, and $1/2$ MIC) of 1 (MIC = $0.75 \mu\text{g/mL}$) (a 75% decrease in MK-8 is seen at $1/2$ MIC); (b) MRSA treated with vancomycin ($2 \mu\text{g/mL}$) and 1 ($0.38 \mu\text{g/mL}$) (treatment with vancomycin and 1 resulted in 10 and 75% decreases in MK-8 levels, respectively). Ctrl (control), untreated cells. *, $p < 0.01$.

Table 3. Thermodynamic Constants for the Binding of CoA and the CoA Adducts of 1 and 6 to *saMenB*

Compound	IC_{50} (μM) ^a	K_d (μM) ^b	$\Delta\Delta G^c$ (kcal/mol)
CoA		25 ± 4	
	4.2 ± 1.6	2.8 ± 0.2	1.3
7			
	7.2 ± 3.0	2.8 ± 0.7	1.3
8			

^a IC_{50} values were determined using the MenE–MenB coupled assay where MenB was rate limiting. In contrast, no inhibition was observed with concentrations of up to $50 \mu\text{M}$ 7 or 8 when MenE was rate limiting in the coupled assay. ^b K_d values for the interaction of compounds with *saMenB* were determined using isothermal titration calorimetry (ITC). In contrast, no binding could be detected with up to $200 \mu\text{M}$ 7 or 8 when ITC was used to analyze the interaction of the compounds with MenE. ^c $\Delta\Delta G$ was determined by calculating ΔG of compound binding vs ΔG of CoA binding (see Table S2 for complete thermodynamic values). All IC_{50} measurements were performed in triplicate, and ITC experiments were performed in duplicate.

M. tuberculosis grown aerobically or in the low oxygen recovery assay, respectively.⁴¹ In addition, whereas compound 1 showed no activity toward *E. coli*, *P. mirabilis*, and *K. pneumoniae* under aerobic growth conditions, MIC values of $12.5 \mu\text{g/mL}$ (*E. coli* and *P. mirabilis*) and $62.5 \mu\text{g/mL}$ (*K. pneumoniae*) were observed under anaerobic conditions. Compound 1 also demonstrated activity toward *H. influenzae* grown under capnophilic conditions (MIC = $0.25 \mu\text{g/mL}$) but showed no activity toward *P. aeruginosa* under either aerobic, capnophilic, or anaerobic conditions. Complementation studies were performed by supplementing the media with $10 \mu\text{M}$ MK-4 or MD, and in organisms for which 1 displayed an MIC, addition of MK-4 resulted in an increase in the MIC value to $>60 \mu\text{g/mL}$.

Although these studies provide strong support that the antibacterial activity of 1 results from a direct effect on MK biosynthesis, we speculated that if 1 did have additional target(s) unrelated to MK biosynthesis, then the lack of activity of 1

against the Gram-negative bacteria that were grown aerobically (i.e., where they utilize Q and not MK) might be due to an inability of the compound to penetrate the bacteria. Thus, we evaluated the activity of 1 against *P. aeruginosa*, *K. pneumoniae*, and *P. mirabilis* under aerobic conditions in the presence of $1/2$ MIC polymyxin B to improve cell permeability.^{50,51} However, this did not alter the whole cell activity of 1, suggesting that the lack of activity was not caused by uptake issues.

1 Reduces MK Level in MRSA. *S. aureus* produces an array of MK species that differ in the length of the isoprenyl chain attached to the naphthoquinone nucleus. In agreement with previous studies, MK-8 (eight isoprenyl units) was found to be the most abundant MK in *S. aureus* (Figure S3).^{24,38,52,53} To analyze the impact of 1 on MK levels in growing cells, the change in MK-8 by treatment of MRSA with 1 was quantified by tandem mass spectrometry using commercially available MK-9 as a standard (Figure 1). Treatment of MRSA cells with increasing

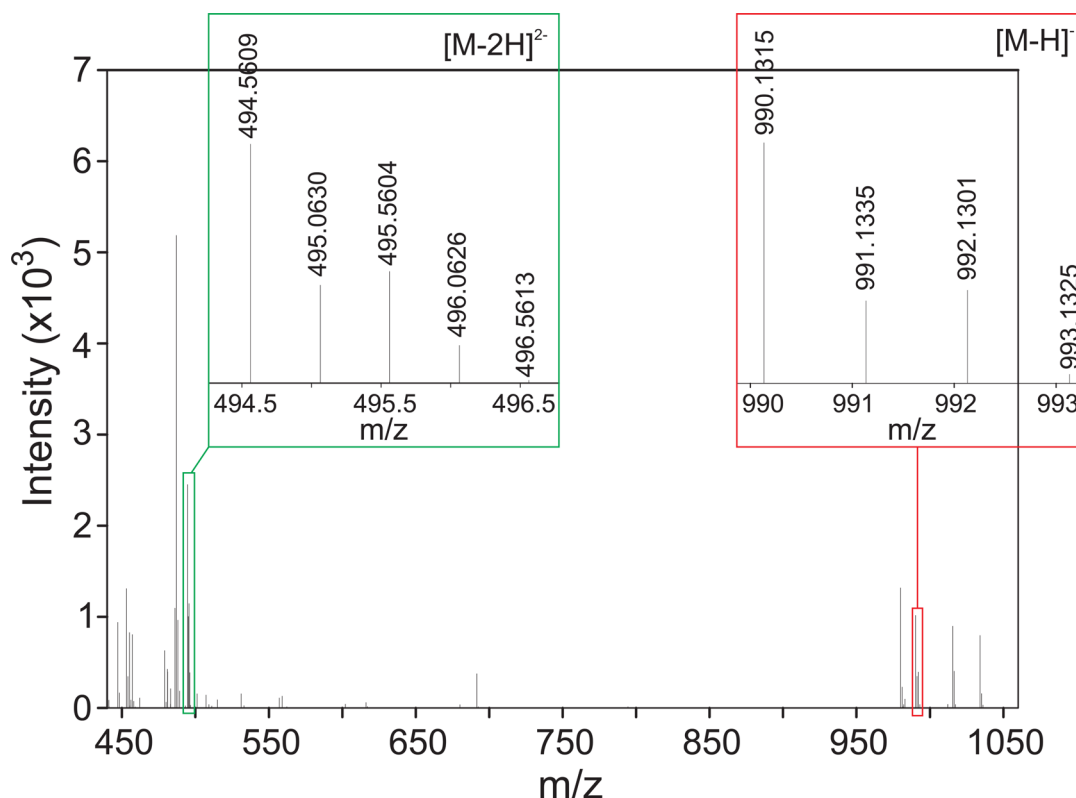


Figure 2. Formation of CoA adduct **8** in MRSA cells treated with **1**. High-resolution LC-UV/MS spectrum of an extract from MRSA cells treated with 8 $\mu\text{g}/\text{mL}$ of **1**. Found-by-formula (FBF) search clearly indicates the presence of **8**, which is the CoA adduct of **1** (m/z 991.1329) but not of **7**, which is the CoA adduct of the corresponding acid (**6**) (m/z 977.1235). Observed peaks correspond to **8** $[\text{M} - \text{H}]^- = 990.1315$ and $[\text{M} - 2\text{H}]^{2-} = 494.5608$. The insets (red and green boxes) show isotopic distribution of $^{35}\text{Cl}/^{37}\text{Cl}$ present in **8** with calculated relative abundance of m/z ions 100, 39, 48, and 16%, respectively, among the four peaks shown for $[\text{M} - \text{H}]^-$ (see Table S1 for complete analysis of theoretical and observed isotopic distribution). Y-axis is relative intensity, and X-axis is counts versus mass-to-charge (m/z).

concentrations of **1** ($1/_{10}$, $1/_{5}$, $1/_{3}$, and $1/_{2}$ MIC) resulted in a dose-dependent decrease in MK-8 (Figure 1a). In addition, whereas $1/_{2}$ MIC of **1** ($0.375 \mu\text{g}/\text{mL}$) reduced the relative amount of MK-8 by 75%, $1/_{2}$ MIC of vancomycin ($2 \mu\text{g}/\text{mL}$) resulted in only a $\sim 10\%$ change, again consistent with a specific effect of **1** on MK biosynthesis (Figure 1b).

1 Forms a CoA Adduct in MRSA-Treated Cells.

Previously, we reported that the 4-oxo-4-phenyl-2-butenates form a CoA adduct in vitro, which is responsible for the inhibition of MenB.⁴¹ We thus speculated that the antibacterial activity of **1** results from the formation of this CoA adduct (**8**) (Table 3) in cells where it may inhibit MenB. Using high-resolution LC-UV/MS we could demonstrate the accumulation of **8** (calculated m/z 991.1392) in treated cells with peaks corresponding to $[\text{M} - \text{H}]^- = 990.1315$ and $[\text{M} - 2\text{H}]^{2-} = 494.5608$ (Figure 2). Isotopic distribution peaks corresponding to the 2 m/z increase due to the presence of Cl in the molecule were also observed: $[\text{M} - \text{H}]^- = 990.1315$ (^{35}Cl) and 992.1300 (^{37}Cl) (Figure 2, inset; Table S1), thus clearly indicating the formation of **8** from treatment of **1** in MRSA cells.

Inhibition of *saMenB* by **8.** Although the presence of **8** in MRSA-treated cells was not unsurprising, we initially hypothesized that the active species would be the acid form **7** because this is a potent inhibitor of *mtMenB* (Figure S2). This hypothesis stemmed from the knowledge that esterification is used as a strategy to protect free carboxylates to facilitate cell penetration after which hydrolysis by endogenous esterases liberates the active pharmacophore.^{54,55} However, using high-resolution LC-UV/MS, we were unable to detect **7** in cell extracts (Figure 2).

We thus explored the ability of **8** and the corresponding acid (**7**) to bind to and inhibit *saMenB* in vitro. Using the MenE–MenB coupled assay,⁵⁶ we discovered that both **7** and **8** inhibit *saMenB* with similar IC_{50} values ($4\text{--}7 \mu\text{M}$, Table 3). In addition, we also used isothermal titration calorimetry (ITC) to quantify binding of **7** and **8** to *saMenB*. The data shown in Figure S4 were fit to a one-site binding model yielding K_d values of $2.8 \mu\text{M}$ for each ligand (Table 3). In comparison, CoA has a K_d value of $25 \mu\text{M}$ for *saMenB*, showing that the acyl group provides an additional 1.3 kcal/mol in binding energy equivalent to the formation of one hydrogen bond between the acyl group and the enzyme ($\Delta\Delta G = 1.3 \text{ kcal/mol}$) (Table S2). Because the inhibition of *saMenB* was assessed using a coupled assay, which involved the generation of the MenB substrate using MenE, we also verified that **7** and **8** did not bind to or inhibit MenE (Table 3).

1 Reduces the Level of DHNA in MRSA Cells. To further probe if **1** directly targets *saMenB* in MRSA, we posited that the substrate of MenB, OSB-CoA, would accumulate in treated cells. The mass spectrum of OSB-CoA has peaks at $[\text{M} - \text{H}]^- = 970.1492$ and $[\text{M} - 2\text{H}]^{2-} = 484.5686$ (Figure S5). However, using this as a standard, we were not able to detect OSB-CoA in extracts from untreated cells or those treated with **1**. We posited that our inability to detect OSB-CoA might be related to the relative instability of this metabolite, which can undergo a nonenzymatic rearrangement leading to the formation of spirodilactone (Scheme 1). However, we were also unable to detect spirodilactone in either treated or untreated cells. We then searched for the downstream product of MenB and determined that levels of DHNA were substantially reduced in MRSA cells

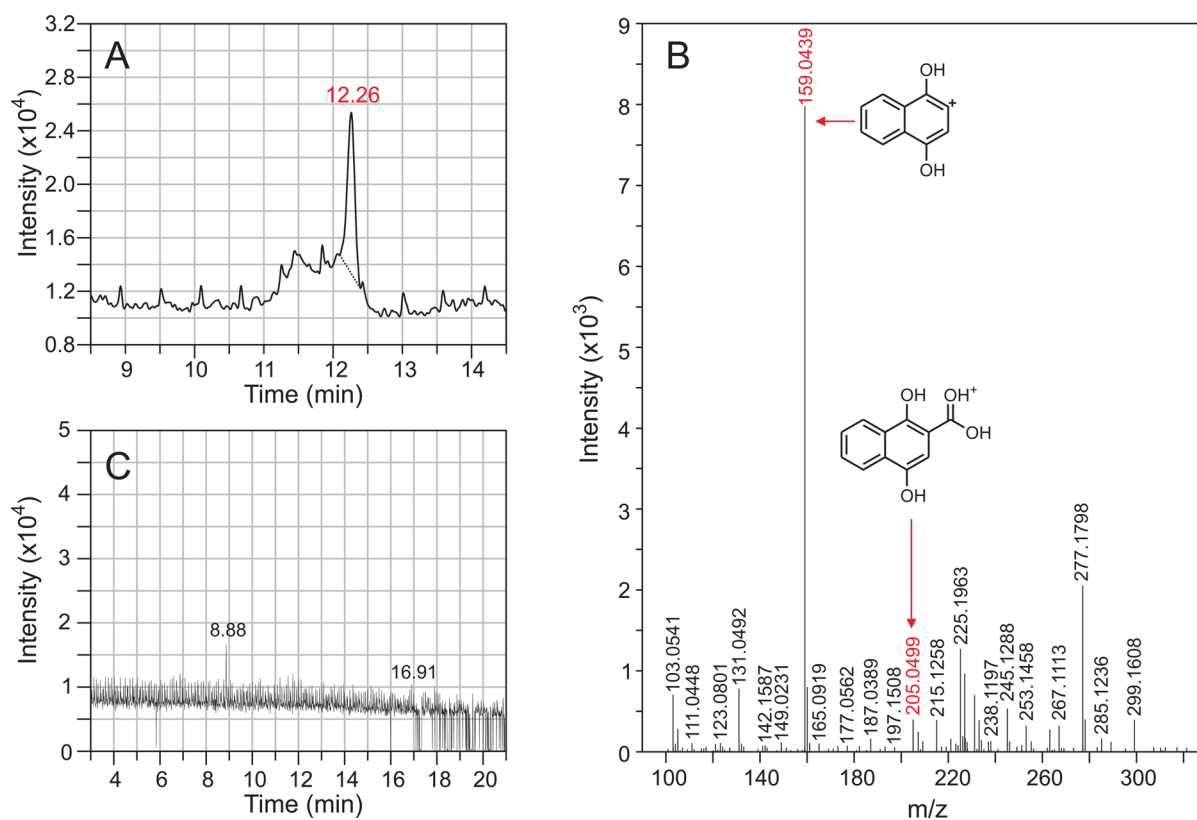


Figure 3. Effect of **1** on the level of DHNA in MRSA cells. High-resolution LC-UV/MS spectra of untreated cells and cells treated with 8 $\mu\text{g}/\text{mL}$ **1**. Commercially available DHNA has a retention time of 12.22 min with $[\text{M} + \text{H}]^+ = 205.0499$ and also m/z 227.0321, $[\text{M} + \text{Na}]^+$, m/z 159.0443 (loss of CO_2), m/z 131.0493 (CO loss), and m/z 103.0546 (CO loss) (see Figure S6 for analysis of commercially available DHNA). (A) In untreated cells, a peak is observed with a retention time of 12.26 min. (B) The mass spectrum of the peak 12.26 min is consistent with DHNA: $\text{ESI}^+ = 205.0499$, 159.0439, 131.049, and 103.055. (C) Using the same protocol, no evidence of DHNA is seen in cells treated with **1**.

treated with **1** (Figure 3). Commercially available DHNA was used as a standard for method development and MS detection. The retention time of DHNA was determined to be 12.22 min with a $[\text{M} + \text{H}]^+$ of 205.0499. DHNA undergoes facile MS fragmentation with the loss of CO_2 to give an m/z 159.0443 ion and also yields ions with m/z 227.0321 ($[\text{M} + \text{Na}]^+$), m/z 131.0493 (loss of CO), and m/z 103.0546 (loss of CO) (Figure S6). Extracts from untreated cells were shown to contain DHNA (retention time, 12.26 min) (Figure 3A) characterized by ESI^+ peaks at m/z 205.0499 ($[\text{M} + \text{H}]^+$), 159.0439, 131.049, and 103.055 (Figure 3B). However, DHNA could not be detected in cells treated with **1** (Figure 3C), supporting a specific effect of **1** on *saMenB*.

MRSA Treated with 1 Forms SCVs and Phenocopies Genetic Disruption of *menB*. Previous studies have shown that genetic defects in the *menB* gene as well as knockout/knockdown of MenB result in the SCV phenotype and that supplementation with exogenous MK-4 or MD can restore the wild-type phenotype.^{24,36} We thus investigated the morphology of MRSA colonies grown on tryptic soy agar (TSA) plates in the presence or absence of **1** (Figure 4). The agar MIC of **1** was found to be 8 $\mu\text{g}/\text{mL}$, which was higher than the broth MIC, a difference often observed for antibacterial compounds.⁵⁷ Growth of MRSA on TSA containing 4 $\mu\text{g}/\text{mL}$ **1** ($1/2$ agar-MIC) showed no colonies after 24 h, in contrast to cells grown in the absence of **1**, whereas small colonies appeared in the presence of **1** after 48 h, consistent with the SCV phenotype. Addition of 10 μM MK-4 to the TSA plates together with 16 $\mu\text{g}/\text{mL}$ **1** ($2\times$ agar-MIC) showed wild-type growth, indicating that MK-4 can abrogate the

antibacterial activity of **1**. Figure 4 also contains data on the growth of a *menB*^{-/-} strain,²⁴ showing the formation of small, pigmentless, slow-growing colonies after 48 h. Thus, treatment of MRSA with sub-MIC concentrations of **1** phenocopies disruption of the *menB* gene.

Complementation of defects in MK biosynthesis by MK-4 or MD has been hypothesized to occur either by directly replacing MK in the electron transport chain or by acting as substrates for the de novo synthesis of MK. To explore these possibilities, we analyzed the MK distribution in MRSA cells treated with **1** and supplemented with either MK-4 or MD (Figure 5). Although MK-4 supplementation did not lead to recovery of the natural MK distribution, addition of MD to the media resulted in a distribution of MK species that closely resembled that observed in the absence of **1** (Figure 5). Thus, for the first time, we can conclude that MD can be used as a precursor for the synthesis of MK by enzyme(s) that are downstream of MenB, possibly as a substrate for MenA, which adds the isoprenyl side chain to the naphthoquinone ring. MK-4, in contrast, can be directly used in oxidative respiration.

1 Shows Promising Antibacterial Activity Against MRSA in Vivo. We evaluated the antibacterial activity of **1** in both systemic and thigh MRSA infection mouse models (Figure 6). Oxacillin served as a negative control for both models because this drug does not have antibacterial activity against MRSA in vitro, whereas vancomycin was used as a positive control (Table 1). In the systemic infection group, control animals that received only vehicle or oxacillin died within 2 days post-infection with an average survival rate of 1.5–1.6 days. In contrast, vancomycin

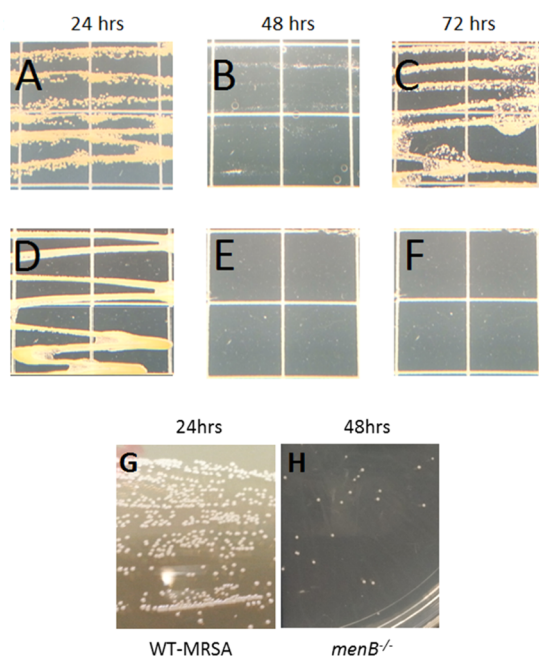


Figure 4. SCV formation following treatment of MRSA cells with **1** or by knocking out *menB*. (A) The normal growth phenotype of wt MRSA cells shows defined individual colonies after 24 h at 37 °C. (B) MRSA plated on TSA containing 4 μg/mL **1** and incubated for 48 h shows SCV morphology that leads to overgrowth after 72 h (C). (D) MRSA plated on TSA containing 16 μg/mL **1** (2× MIC) and 10 μg/mL MK-4 shows overgrowth after 24 h of incubation, indicating that MK complements the antibacterial activity of **1**. (E, F) No growth is seen even after 72 h of incubation on TSA with 8 μg/mL **1**, making this concentration the agar-MIC. (G, H) Comparison of *S. aureus* growth upon knockout of the *menB* gene.²⁴ Consistent with other studies, the *menB*^{-/-} strain²⁴ forms SCVs characterized by loss of pigmentation and small/slow growing colonies.

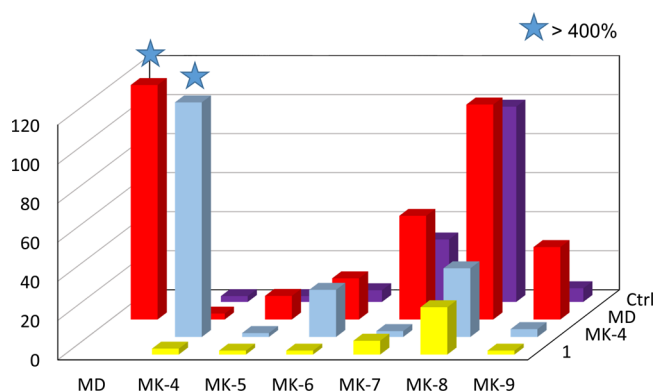


Figure 5. Menaquinone (MK) quantification in MRSA cells treated with **1** and supplemented with menaquinone-4 (MK-4) or menadiione (MD). Untreated cells show a distribution of MKs that vary in the length of the polyisoprene chain and in which MK-8 is the dominant species. Treatment with **1** (0.38 μg/mL) results in a decrease in all MK species. Cells supplemented with MD (10 μM) but not MK-4 (10 μM) recover the MK distribution observed in untreated cells. This indicates that MD may act as a substrate for MK biosynthesis downstream of the enzyme inhibited by **1**. Presumably MK4 directly replaces the function of MK-8 and the other major MK species in the electron transport chain. Because MK-4 and MD were supplemented at 10 μM, the levels of these molecules were >400% relative to MK-8 levels in untreated cells.

increased the survival rate up to 5.8 days post-infection. Promisingly, treatment with 100 mg/kg **1** resulted in a survival

rate of 4.6 days ($p < 0.005$) (Figure 6a). In addition, increasing concentrations of **1** resulted in a dose-dependent reduction in bacterial burden in the thigh model of infection, with 100 mg/kg reducing bacterial load by 3.1 log colony-forming units (CFU)/g tissue (Figure 6b). This contrasted with only a minimal effect of oxacillin on bacterial load, whereas vancomycin caused a reduction of 4.2 log CFU/g of tissue. Thus, **1** demonstrates promising in vivo efficacy using both systemic and thigh models of MRSA infection.

OUTLOOK AND CONCLUSIONS

Previously, we performed an HTS to identify inhibitors of MenB, the 1,4-dihydroxynaphthoyl-CoA synthetase in the bacterial MK pathway. This HTS yielded several classes of inhibitors including a series of 2-amino-4-oxo-4-phenylbutanoates. We subsequently demonstrated that the 2-aminobutanoates eliminated the amino group, yielding the corresponding butenoate which then reacts with CoA to form an adduct that inhibits MenB. Although the butenoic acids have poor antibacterial activity, the methyl ester derivatives have potent activity, suggesting that the lack of activity of the butenoic acids results from poor penetration into the cell. In the present work, we have expanded our studies to explore the mode of action of the methyl butenoates in *S. aureus*. Methyl 4-oxo-4-(4-chlorophenyl)-2-butenoate **1** has potent activity against the human pathogen *M. tuberculosis* (MIC = 0.64 μg/mL). Here, we show that **1** also has potent antibacterial activity against MSSA and MRSA, as well as other MK-utilizing bacteria. We also provide compelling evidence that the activity of **1** results from a direct effect on MK biosynthesis through inhibition of *saMenB* (Figure 7). We show that **1** can penetrate into MRSA cells and form a CoA adduct that is an inhibitor of *saMenB*. Treatment with **1** depletes DHNA levels, reduces MK, and ultimately results in the formation of the SCV growth phenotype, thus phenocopying a *menB*^{-/-} knockout strain.²⁴ The growth defects caused by **1** can be recovered by the addition of MK-4 or MD to the media, and we demonstrate that complementation with MD results from conversion of this compound into MK. Finally, given the potent in vitro activity of **1**, we evaluated the in vivo efficacy of this compound in two mouse models of MRSA infection and showed that **1** increases survival time and reduces bacterial load. These studies thus validate the MK biosynthesis pathway as a target for the development of novel antibacterial agents.

Although **1** is a useful chemical tool for exploring the role of MenB and MK biosynthesis in bacterial growth and survival, it is likely that **1** also reacts with other nucleophiles in the cell. Improvements in the selectivity of compounds derived from **1** can be envisaged on the basis of elegant approaches that have been applied to the generation of selective covalent kinase inhibitors including compounds that target Bruton's tyrosine kinase (BTK)⁵⁸ such as ibrutinib⁵⁹ and CC-292,⁶⁰ as well as the reversible covalent cyanoacrylamides developed by Taunton and co-workers.^{61,62} In this regard, the observation that CoA can bind to MenB suggests that modifications that reduce the electrophilicity of the Michael acceptor while increasing the affinity of **1** for the enzyme might lead to compounds that inhibit MenB through the formation of the CoA adduct on the enzyme. In addition, it is known that variation in the substitution of the phenyl ring in the 4-oxo-4-phenyl-2-aminobutanoates alters the rate at which the amine is eliminated from these compounds,⁴¹ and such changes are also envisaged to alter the stability of the corresponding thiol adducts. Thus, the reversible covalent formation of CoA adducts that are stabilized by MenB might

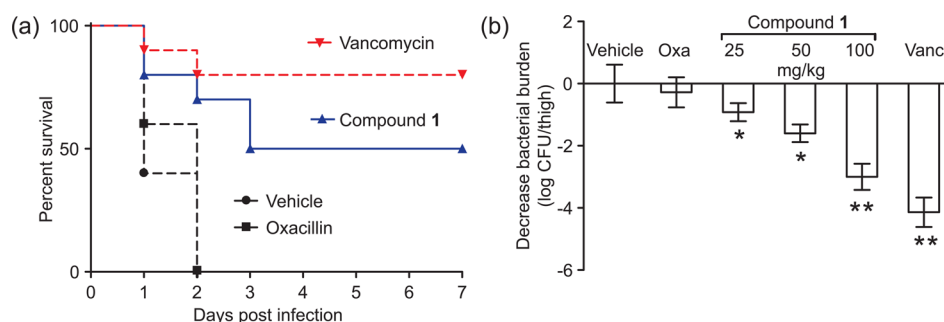


Figure 6. In vivo antibacterial efficacy of compound **1** against MRSA: (a) survival of infected mice treated with vehicle (black circles, $n = 5$), oxacillin (100 mg/kg, black squares, $n = 5$), compound **1** (100 mg/kg, blue triangles, $n = 10$) or vancomycin (100 mg/kg, red triangles, $n = 10$); (b) decrease of bacterial burden in thigh muscle after treatment with vehicle ($n = 3$), oxacillin (Oxa, 100 mg/kg, $n = 3$), compound **1** (25, 50, and 100 mg/kg, $n = 5$), and vancomycin (Vanc, 100 mg/kg, $n = 3$). Statistical significance was determined using a one-tailed t test where * indicates $p < 0.05$ and ** indicates $p < 0.005$.

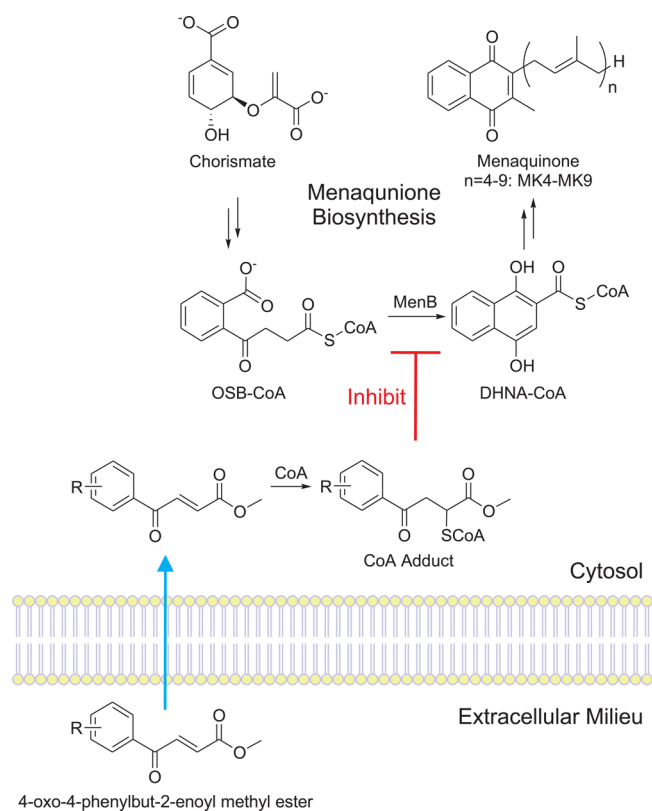


Figure 7. Proposed mode of action of the 4-oxo-4-phenylbut-2-enoyl methyl esters. Upon penetration into the cell, the corresponding CoA adduct is formed, leading to inhibition of MenB and a decrease in the levels of DHNA and MK.

also provide a strategy for improving the selectivity of molecules that target MenB.

MATERIALS AND METHODS

Compounds. Chemicals were obtained from commercial vendors and used without further purification. The compounds tested for activity were available from previous studies.⁴¹ The CoA adduct of methyl 4-oxo-4-(4-chlorophenyl)-2-butenoyl (8) was prepared as follows: a solution of CoA (0.1 mmol) in water (1.5 mL) was added to a solution of methyl 4-oxo-4-(4-chlorophenyl)-2-butenoyl (0.5 mmol) in anhydrous DMSO (1 mL) at room temperature. The resulting mixture was stirred at room temperature for 4 h, after which the reaction was quenched

by the addition of formic acid (0.1%, 0.5 mL). The product was purified by HPLC using a Shimadzu 20AB instrument with a Phenomenex C18, 5 μ m, 250 \times 10 mm semipreparative column and by running a gradient of 0–40% acetonitrile in water over 40 min at a flow rate of 4 mL. The product eluted at 15 min and was obtained by lyophilization. ESI⁻ calculated for $[M - H]^-$ C₃₂H₄₅ClN₇O₁₉P₃S (compound **8**): 990.13, found 990.2 (Figure S7).

S. aureus MenB (saMenB). The gene encoding MenB was cloned from MRSA (Rosenbach, ATCC BAA-1762) into a pET28a⁺ plasmid so that a 6x-HIS tag was encoded at the N-terminus. The expression and purification of saMenB followed a method similar to that described previously for *E. coli* MenB.⁴⁶ Briefly, protein expression was induced with 0.5 mM IPTG when the OD₆₀₀ of the culture reached 0.55, after which the culture was shaken overnight at 22 °C. Cells were collected by centrifugation, resuspended in 20 mM sodium phosphate buffer, pH 8.5, containing 250 mM NaCl, 1 mM MgCl₂ and protease inhibitor cocktail, and then lysed by passing the suspension twice through a cell disruptor (35 kpsi). Following ultracentrifugation, saMenB was purified from the supernatant by affinity chromatography with HIS bind resin and by running an imidazole gradient from 20 to 500 mM. Fractions containing saMenB were pooled and chromatographed on a Sephadex 75 column using 20 mM sodium phosphate buffer, pH 8.5, containing 250 mM NaCl and 1 mM MgCl₂ as the eluent to rapidly remove imidazole. The protein was concentrated to ~40 μ M ($\epsilon_{280} = 33140 \text{ M}^{-1} \text{ cm}^{-1}$) and stored at -80 °C.

Kinetic Assays. Enzyme inhibition studies were performed in 20 mM sodium phosphate buffer, pH 8.5, containing 250 mM NaCl and 1 mM MgCl₂ using a MenE–MenB coupled assay in which saMenB was rate-limiting.⁴⁷ IC₅₀ values were determined in reaction mixtures containing *o*-succinylbenzoate (60 μ M), ATP (120 μ M), CoA (120 μ M), saMenB (0.1 μ M), and various inhibitor concentrations (0.05–250 μ M). Reactions were initiated by the addition of ecMenE (5 μ M) with or without 1 h of incubation in 37 °C, and the production of DHNA-CoA was monitored at 392 nm ($\epsilon_{392} = 4000 \text{ M}^{-1} \text{ cm}^{-1}$).

Isothermal Titration Calorimetry. ITC was used to quantify the affinity of CoA and the CoA adducts **7** and **8** for saMenB using a Micro-Cal VP-ITC instrument. Aliquots of 2 mM ligand (4 or 8 μ L) were titrated into a solution of 25 μ M saMenB (1.8 mL) using a 12–20 s titration period with 300 s between each titration. Lyophilized ligands were dissolved in the same buffer as that used for the enzyme (20 mM sodium

phosphate buffer, pH 8.5, containing 250 mM NaCl and 1 mM MgCl₂). ITC experiments were performed at 22 °C.

Bacterial Strains and Antibacterial Assays. Bacterial strains used in this study included methicillin-sensitive (MSSA, ATCC 25923) and -resistant (MRSA, BAA 1762) *S. aureus*, *E. coli* (ATCC 25922), *Bacillus subtilis* (ATCC 6051), *Haemophilus influenzae* (ATCC 49427), *Enterococcus faecium* (ATCC 19434), *Klebsiella pneumoniae* (ATCC 13883), *Proteus mirabilis* (ATCC 35659), *Pseudomonas aeruginosa* (ATCC 27853), and *Mycobacterium smegmatis* (ATCC 700084). Minimum inhibitory concentrations (MICs) were determined using visual inspection of cells grown in transparent 96-well plates. Bacteria were grown to mid log phase (OD₆₀₀ of 0.6–0.8) in Mueller–Hinton broth, tryptic soy broth, or 7H9 media at 37 °C in an orbital shaker. A final inoculum concentration of 10⁶ CFU/mL per well was treated with inhibitor in a 2-fold dilution series at concentrations ranging from 0.06 to 125 μg/mL. MIC values under capnophilic conditions were obtained in a humidified candle jar and using a candle to obtain (~8% O₂). GasPak EZ Anaerobe Sachets (BD 260001) were used to obtain anaerobic conditions (<0.1% O₂). The MIC was defined as the minimum concentration (modal value) at which no obvious growth was observed after 24–72 h of incubation at 37 °C. Complementation studies were performed by supplementing synthetic broth with 10 μM menaquinone-4 (MK4) or 10 μM menadione (MD).

Quantification of MK Levels. MK was extracted from *S. aureus* cells using a liquid–liquid extraction method.^{63,64} A 100 mL starter culture of MRSA in Mueller–Hinton-II (MH-II) broth was treated with 1/2 MIC of vancomycin (2 μg/mL) or 1 (0.38 μg/mL). Cultures were incubated at 37 °C in an orbital shaker to late-log phase (OD₆₀₀ between 0.9 and 1.0) and then diluted with MH-II broth to 10⁹ cells/mL. Cells were isolated from 100 mL of culture by centrifugation (5000 rpm, 30 min) and then resuspended in 30 mL of phosphate buffer (50 mM KH₂PO₄, pH 7.0). The suspension was extracted with 20:15 mL of methanol/chloroform. The lower organic layer was collected, washed with brine (30 mL), and dried with MgSO₄ prior to MS/MS analysis. MK quantification was conducted using a flow injection analysis (FIA)–atmospheric-pressure chemical ionization (APCI)–MS/MS system and a TSQ Quantum Access triple-quadrupole mass spectrometer. Briefly, 5 μL of sample was loop injected, and the flow was directed to the APCI source. Mass spectrometry was performed in positive ion mode with 3.5 kV, gas pressure of 30 psi, and a capillary temperature of 350 °C. Multiple reaction monitoring (MRM)^{65,66} transitions were detected at 100 ms dwell times. Multiple injections were performed over a 5 min time frame. MK-9 was used as a standard for generating a calibration curve. Complementation studies were performed by supplementing synthetic broth with 10 μM menaquinone-4 (MK4) or 10 μM menadione (MD).

Sample Analyses by LC-UV/MS. DHNA. High-resolution LC-UV/MS analysis was performed on samples prepared as follows.^{67,68} MRSA was grown to an OD₆₀₀ of 1 after which 1 mL of the culture was filtered using a sterile Millipore filter to capture the cells. The filter was transferred to MH-II agar plates where the cells were cultured with or without 8 μg/mL **1** for 18 h. Cells were harvested from the filter, lysed by bead-beating, and centrifuged in a SpinX column. Samples of the supernatant were analyzed by high-resolution LC-UV/MS (ESI⁺, *m/z* 100–3200) using an Agilent LC-UV-TOF mass spectrometer (G6224A oaTOF). The LC was performed using a Kinetex XB-C18 column (100 Å, 2.6 μm, 150 × 2.1 mm) with 0.1% HOAc/H₂O

(solvent A) and CH₃OH (solvent B) at 45 °C. The flow rate was 0.40 mL/min, and the amount of solvent B was as follows: 0–2 min, 5% B; 2–32 min, 5–95% B; 32–35 min, 95–96% B. Sample volumes were 5 μL for the synthetic standards and 20 μL for the sample supernatants.

CoA Derivatives. High-resolution LC-UV/MS analysis was performed on samples prepared as described above. The supernatant was centrifuged using a SpinX column and the filtrate lyophilized. Samples were analyzed by high-resolution LC-UV/MS (ESI⁻, *m/z* 100–3200) using an Agilent LC-UV-TOF mass spectrometer (G6224A oaTOF). The LC was performed using a Kinetex HILIC column (100 Å, 2.6 μm, 150 × 2.1 mm) with H₂O/CH₃CN 1:1 (10 mM AmAc, 0.02% Ac) (solvent A) and CH₃CN/H₂O, 95:5 (10 mM AmAc, 0.02% Ac) (solvent B) at 30 °C. The flow rate was 0.50 mL/min, and the amount of solvent B was as follows: 0–2 min, 96% B; 2–22.5 min, 96–0% B; 32–35 min, 0% B. Sample volumes were 5 μL for the synthetic standards and 25 μL for the sample supernatants.

Colony Morphology. The colony morphology was analyzed by plating MRSA cells on tryptic soy agar (TSA) media with or without **1**. A single colony of MRSA was streaked on a 20 mL TSA plate containing 0, 4, or 8 μg/mL **1**. For the rescue experiments, TSA plates contained 16 μg/mL **1** and 10 μM MK-4 or MD. Plates were incubated for up to 84 h at 37 °C. In addition to the slow-growth phenotype, SCV colonies were also nonpigmented (colorless) in contrast to rapidly growing wild-type yellow colonies.⁶⁹

In Vivo Antibacterial Activity of 1. All animals were maintained in accordance with the American Association for Accreditation of Laboratory Animal Care criteria, and criteria were reviewed and approved by SBU IACUC. Experiments were conducted under BSL-2 conditions in the Division of Laboratory Animal Resources at Stony Brook University. AVMA guidelines on euthanasia after the experiments were followed at the end of each experiment. Six-week-old male Swiss Webster mice (Taconic) were used. Systemic infection was induced by intraperitoneal (ip) injection of 2 × 10⁷ CFU MRSA in 200 μL of saline. Drug doses, including vancomycin and oxacillin, were prepared in a vehicle consisting of 40% saline, 40% ethanol, and 20% PEG-400 and were delivered by subcutaneous injection (sc) at 1, 12, and 24 h post-infection at a dose of 100 mg/kg. Mortality was checked every 12 h for 7 days. For the thigh infection model, mice were rendered neutropenic by injecting cyclophosphamide (CPA) 4 days (ip, 150 mg/kg) and 1 day (ip, 100 mg/kg) before infection. Thigh infections were performed by injecting MRSA cells (10⁶ CFU in 50 μL of saline) into the left thigh muscle (intramuscular, im). All drugs, including vancomycin and oxacillin, were administered by sc injection 1 and 12 h post-infection at a dose of 100 mg/kg (vancomycin and oxacillin) or 100, 50, and 25 mg/kg (compound **1**). Infected thigh muscles were collected, weighed, and homogenized in 2 mL of saline. Serial dilutions of each homogenized sample were plated on Mueller–Hinton agar supplemented with 5% sheep blood. The number of colony-forming units (CFU) was determined following overnight incubation, and the bacterial burden was determined. Statistical significance was determined using a one-tailed *t* test.

■ ASSOCIATED CONTENT

📄 Supporting Information

The Supporting Information is available free of charge on the ACS Publications website at DOI: 10.1021/acsinfecdis.6b00023.

Comparison of theoretical vs observed ion isotopic distribution of **8**; thermodynamic constants for the binding of CoA and CoA adducts **7** and **8** to *saMenB*; role of menaquinone (MK) in the electron transport chain; 4-oxo-4-phenylbutanoic acids are able to mimic the transition state of the MenB reaction by forming CoA adducts through a Michael addition reaction; menaquinone quantification in MRSA treated with $1/2$ MIC of antibacterial agents; ITC binding thermographs; high-resolution LC-UV/MS ESI⁻ of OSB-CoA; LC/ESI⁺ chromatograms for DHNA standard; NMR and MS of compound **8** (PDF)

AUTHOR INFORMATION

Corresponding Author

* (P.J.T.) E-mail: peter.tonge@stonybrook.edu. Phone: (631) 632-7907.

Author Contributions

[†]J.S.M. and Y.L. contributed equally to this work.

Funding

This work was supported by NIH Grants GM102864 to P.J.T. and GM100477 and by a W. Burghardt Turner Fellowship to J.S.M.

Notes

The authors declare no competing financial interest.

ACKNOWLEDGMENTS

We thank Dr. Robert Rieger from the Proteomics Center at Stony Brook University for assistance with MK quantification and analysis and Dr. Eric Skaar from Vanderbilt University for his generous gift of the *menB*^{-/-} *S. aureus* strain.

ABBREVIATIONS USED

MRSA, methicillin-resistant *Staphylococcus aureus*; MSSA, methicillin-sensitive *Staphylococcus aureus*; MK, menaquinone; DHNA, 1,4-dihydroxy-2-naphthoic acid; OSB-CoA, *o*-succinylbenzoyl-coenzyme A; MIC, minimum inhibitory concentration; SCV, small-colony variant; MD, menadione; TSA/B, tryptic soy agar/broth; CFU, colony-forming units

REFERENCES

- Li, K., Schurig-Briccio, L. A., Feng, X., Upadhyay, A., Pujari, V., Lechartier, B., Fontes, F. L., Yang, H., Rao, G., Zhu, W., Gulati, A., No, J. H., Cintra, G., Bogue, S., Liu, Y. L., Molohon, K., Orlean, P., Mitchell, D. A., Freitas-Junior, L., Ren, F., Sun, H., Jiang, T., Li, Y., Guo, R. T., Cole, S. T., Gennis, R. B., Crick, D. C., and Oldfield, E. (2014) Multitarget drug discovery for tuberculosis and other infectious diseases. *J. Med. Chem.* 57, 3126–3139.
- Fischbach, M. A., and Walsh, C. T. (2009) Antibiotics for emerging pathogens. *Science* 325, 1089–1093.
- West, K. (1993) Methicillin-resistant *Staph aureus*. In this era of resistant organisms, it's vitally important for you to comply with the infection-control procedures set forth by the CDC. *Emerg Med. Serv* 22 (70–71), 78.
- Kessler, R. (2012) Superbug hideout: finding MRSA in U.S. wastewater treatment plants. *Environ. Health Perspect.* 120, A437.
- McKenna, M. (2012) Vaccine development: Man vs MRSA. *Nature* 482, 23–25.
- CDC: hospitals “need to do more” to control MRSA. AHRQ report disheartening. *Hosp. Peer Rev.* 2008, 33 (5–6), 11.
- Camins, B. C., and Fraser, V. J. (2005) Reducing the risk of health care-associated infections by complying with CDC hand hygiene guidelines. *Jt. Commission J. Qual. Patient Saf.* 31, 173–179.

- Rosenberg Goldstein, R. E., Micallef, S. A., Gibbs, S. G., Davis, J. A., He, X., George, A., Kleinfelder, L. M., Schreiber, N. A., Mukherjee, S., Sapkota, A., Joseph, S. W., and Sapkota, A. R. (2012) Methicillin-resistant *Staphylococcus aureus* (MRSA) detected at four U.S. wastewater treatment plants. *Environ. Health Perspect.* 120, 1551–1558.

- Barrado, L., Branas, P., Rojo, P., Gomez-Gonzalez, C., Barrios, M., Orellana, M. A., and Chaves, F. (2014) Molecular epidemiology of *Staphylococcus aureus* bacteremia in children, Spain: low risk of methicillin resistance. *J. Infect.* 68, 195–198.

- Jones, M., Huttner, B., Leecaster, M., Huttner, A., Damal, K., Tanner, W., Nielson, C., Rubin, M. A., Goetz, M. B., Madaras-Kelly, K., and Samore, M. H. (2014) Does universal active MRSA surveillance influence anti-MRSA antibiotic use? A retrospective analysis of the treatment of patients admitted with suspicion of infection at Veterans Affairs Medical Centers between 2005 and 2010. *J. Antimicrob. Chemother.* 69, 3401–3408.

- Kalenic, S., Pal, M. P., Palcevski, V. V., Horvatic, J., Mestrovic, T., Barsic, B., Stamenic, V., Burcar, I., Korusic, A., Vucic, M., Civljak, R., Stancic, M., and Budimir, A. (2010) [Guidelines for prevention, control and treatment of infections caused by methicillin-resistant *Staphylococcus aureus* (MRSA): changes and updates of chapter 7.0: treatment of patients with MRSA infection]. *Lijec Vjesn* 132, 340–344.

- Gould, I. M. (2010) VRSA-doomsday superbug or damp squib? *Lancet Infect. Dis.* 10, 816–818.

- Aguado, J. M., San-Juan, R., Lalueza, A., Sanz, F., Rodriguez-Otero, J., Gomez-Gonzalez, C., and Chaves, F. (2011) High vancomycin MIC and complicated methicillin-susceptible *Staphylococcus aureus* bacteremia. *Emerging Infect. Dis.* 17, 1099–1102.

- Malone, J. G. (2015) Role of small colony variants in persistence of *Pseudomonas aeruginosa* infections in cystic fibrosis lungs. *Infect. Drug Resist.* 8, 237–247.

- Haussler, S., Rohde, M., and Steinmetz, I. (1999) Highly resistant *Burkholderia pseudomallei* small colony variants isolated in vitro and in experimental melioidosis. *Med. Microbiol. Immunol.* 188, 91–97.

- Clowes, R. C., and Rowley, D. (1955) Genetic studies on small-colony variants of *Escherichia coli* K-12. *J. Gen. Microbiol.* 13, 461–473.

- Wellinghausen, N., Chatterjee, I., Berger, A., Niederfuehr, A., Proctor, R. A., and Kahl, B. C. (2009) Characterization of clinical *Enterococcus faecalis* small-colony variants. *J. Clin. Microbiol.* 47, 2802–2811.

- Proctor, R. A., Kriegeskorte, A., Kahl, B. C., Becker, K., Loffler, B., and Peters, G. (2014) *Staphylococcus aureus* small colony variants (SCVs): a road map for the metabolic pathways involved in persistent infections. *Front. Cell. Infect. Microbiol.* 4, 99.

- Sendi, P., and Proctor, R. A. (2009) *Staphylococcus aureus* as an intracellular pathogen: the role of small colony variants. *Trends Microbiol.* 17, 54–58.

- Sendi, P., Banderet, F., Graber, P., and Zimmerli, W. (2011) Periprosthetic joint infection following *Staphylococcus aureus* bacteremia. *J. Infect.* 63, 17–22.

- Sendi, P., Rohrbach, M., Graber, P., Frei, R., Ochsner, P. E., and Zimmerli, W. (2006) *Staphylococcus aureus* small colony variants in prosthetic joint infection. *Clin. Infect. Dis.* 43, 961–967.

- Kaech, C., Elzi, L., Sendi, P., Frei, R., Laifer, G., Bassetti, S., and Fluckiger, U. (2006) Course and outcome of *Staphylococcus aureus* bacteraemia: a retrospective analysis of 308 episodes in a Swiss tertiary-care centre. *Clin. Microbiol. Infect.* 12, 345–352.

- Garcia, L. G., Lemaire, S., Kahl, B. C., Becker, K., Proctor, R. A., Denis, O., Tulkens, P. M., and Van Bambeke, F. (2013) Antibiotic activity against small-colony variants of *Staphylococcus aureus*: review of in vitro, animal and clinical data. *J. Antimicrob. Chemother.* 68, 1455–1464.

- Wakeman, C. A., Hammer, N. D., Stauff, D. L., Attia, A. S., Anzaldi, L. L., Dikalov, S. I., Calcutt, M. W., and Skaar, E. P. (2012) Menaquinone biosynthesis potentiates haem toxicity in *Staphylococcus aureus*. *Mol. Microbiol.* 86, 1376–1392.

- Kriegeskorte, A., Grubmuller, S., Huber, C., Kahl, B. C., von Eiff, C., Proctor, R. A., Peters, G., Eisenreich, W., and Becker, K. (2014) *Staphylococcus aureus* small colony variants show common metabolic

features in central metabolism irrespective of the underlying auxotrophism. *Front. Cell. Infect. Microbiol.* 4, 141.

(26) Kahl, B. C., Belling, G., Becker, P., Chatterjee, I., Wardecki, K., Hilgert, K., Cheung, A. L., Peters, G., and Herrmann, M. (2005) Thymidine-dependent *Staphylococcus aureus* small-colony variants are associated with extensive alterations in regulator and virulence gene expression profiles. *Infect. Immun.* 73, 4119–4126.

(27) Gomez-Gonzalez, C., Acosta, J., Villa, J., Barrado, L., Sanz, F., Orellana, M. A., Otero, J. R., and Chaves, F. (2010) Clinical and molecular characteristics of infections with CO₂-dependent small-colony variants of *Staphylococcus aureus*. *J. Clin. Microbiol.* 48, 2878–2884.

(28) Garcia, L. G., Lemaire, S., Kahl, B. C., Becker, K., Proctor, R. A., Denis, O., Tulkens, P. M., and Van Bambeke, F. (2012) Pharmacodynamic evaluation of the activity of antibiotics against hemin- and menadione-dependent small-colony variants of *Staphylococcus aureus* in models of extracellular (broth) and intracellular (THP-1 monocytes) infections. *Antimicrob. Agents Chemother.* 56, 3700–3711.

(29) Sasarman, A., Surdeanu, M., Portelance, V., Dobardzic, R., and Sonea, S. (1971) Classification of vitamin K-deficient mutants of *Staphylococcus aureus*. *J. Gen. Microbiol.* 65, 125–130.

(30) Sasarman, A., Surdeanu, M., Portelance, V., Dobardzic, R., and Sonea, S. (1969) Vitamin K-deficient mutants of bacteria. *Nature* 224, 272.

(31) Kriegeskorte, A., Lore, N. I., Bragonzi, A., Riva, C., Kelkenberg, M., Becker, K., Proctor, R. A., Peters, G., and Kahl, B. C. (2015) Thymidine-dependent *Staphylococcus aureus* small-colony variants are induced by trimethoprim-sulfamethoxazole (SXT) and have increased fitness during SXT challenge. *Antimicrob. Agents Chemother.* 59, 7265–7272.

(32) Sherris, J. C. (1952) Two small colony variants of *Staph. aureus* isolated in pure culture from closed infected lesions and their carbon dioxide requirements. *J. Clin. Pathol.* 5, 354–355.

(33) McNamara, P. J., and Proctor, R. A. (2000) *Staphylococcus aureus* small colony variants, electron transport and persistent infections. *Int. J. Antimicrob. Agents* 14, 117–122.

(34) Dean, M. A., Olsen, R. J., Long, S. W., Rosato, A. E., and Musser, J. M. (2014) Identification of point mutations in clinical *Staphylococcus aureus* strains that produce small-colony variants auxotrophic for menadione. *Infect. Immun.* 82, 1600–1605.

(35) Garcia, L. G., Lemaire, S., Kahl, B. C., Becker, K., Proctor, R. A., Tulkens, P. M., and Van Bambeke, F. (2012) Intracellular forms of menadione-dependent small-colony variants of methicillin-resistant *Staphylococcus aureus* are hypersusceptible to beta-lactams in a THP-1 cell model due to cooperation between vacuolar acid pH and oxidant species. *J. Antimicrob. Chemother.* 67, 2873–2881.

(36) Lannergard, J., von Eiff, C., Sander, G., Cordes, T., Seggewiss, J., Peters, G., Proctor, R. A., Becker, K., and Hughes, D. (2008) Identification of the genetic basis for clinical menadione-auxotrophic small-colony variant isolates of *Staphylococcus aureus*. *Antimicrob. Agents Chemother.* 52, 4017–4022.

(37) von Eiff, C., McNamara, P., Becker, K., Bates, D., Lei, X. H., Ziman, M., Bochner, B. R., Peters, G., and Proctor, R. A. (2006) Phenotype microarray profiling of *Staphylococcus aureus* menD and hemB mutants with the small-colony-variant phenotype. *J. Bacteriol.* 188, 687–693.

(38) Meganathan, R., Kwon, O. Biosynthesis of menaquinone (vitamin K) and ubiquinone (coenzyme Q). *EcoSal Plus* 2009, 3.10.1128/ecosalplus.3.6.3.3

(39) Meganathan, R. (2001) Biosynthesis of menaquinone (vitamin K2) and ubiquinone (coenzyme Q): a perspective on enzymatic mechanisms. *Vitam. Horm.* 61, 173–218.

(40) Matarlo, J. S., Evans, C. E., Sharma, I., Lavaud, L. J., Ngo, S. C., Shek, R., Rajashankar, K. R., French, J. B., Tan, D. S., and Tonge, P. J. (2015) Mechanism of MenE inhibition by acyl-adenylate analogues and discovery of novel antibacterial agents. *Biochemistry* 54, 6514–6524.

(41) Li, X., Liu, N., Zhang, H., Knudson, S. E., Li, H. J., Lai, C. T., Simmerling, C., Slayden, R. A., and Tonge, P. J. (2011) CoA adducts of 4-oxo-4-phenylbut-2-enoates: inhibitors of MenB from the *M. tuber-*

culosis menaquinone biosynthesis pathway. *ACS Med. Chem. Lett.* 2, 818–823.

(42) Li, X., Liu, N., Zhang, H., Knudson, S. E., Slayden, R. A., and Tonge, P. J. (2010) Synthesis and SAR studies of 1,4-benzoxazine MenB inhibitors: novel antibacterial agents against *Mycobacterium tuberculosis*. *Bioorg. Med. Chem. Lett.* 20, 6306–6309.

(43) Debnath, J., Siricilla, S., Wan, B., Crick, D. C., Lenaerts, A. J., Franzblau, S. G., and Kurosu, M. (2012) Discovery of selective menaquinone biosynthesis inhibitors against *Mycobacterium tuberculosis*. *J. Med. Chem.* 55, 3739–3755.

(44) Kurosu, M., and Crick, D. C. (2009) MenA is a promising drug target for developing novel lead molecules to combat *Mycobacterium tuberculosis*. *Med. Chem.* 5, 197–207.

(45) Zhang, Y. J., Ioerger, T. R., Huttenhower, C., Long, J. E., Sasseti, C. M., Sacchetti, J. C., and Rubin, E. J. (2012) Global assessment of genomic regions required for growth in *Mycobacterium tuberculosis*. *PLoS Pathog.* 8, e1002946.

(46) Li, H. J., Li, X., Liu, N., Zhang, H., Truglio, J. J., Mishra, S., Kisker, C., Garcia-Diaz, M., and Tonge, P. J. (2011) Mechanism of the intramolecular Claisen condensation reaction catalyzed by MenB, a crotonase superfamily member. *Biochemistry* 50, 9532–9544.

(47) Truglio, J. J., Theis, K., Feng, Y., Gajda, R., Machutta, C., Tonge, P. J., and Kisker, C. (2003) Crystal structure of *Mycobacterium tuberculosis* MenB, a key enzyme in vitamin K2 biosynthesis. *J. Biol. Chem.* 278, 42352–42360.

(48) Ulaganathan, V., Agacan, M. F., Buetow, L., Tulloch, L. B., and Hunter, W. N. (2007) Structure of *Staphylococcus aureus* 1,4-dihydroxy-2-naphthoyl-CoA synthase (MenB) in complex with acetoacetyl-CoA. *Acta Crystallogr., Sect. F: Struct. Biol. Cryst. Commun.* 63, 908–913.

(49) Sun, Y., Song, H., Li, J., Li, Y., Jiang, M., Zhou, J., and Guo, Z. (2013) Structural basis of the induced-fit mechanism of 1,4-dihydroxy-2-naphthoyl coenzyme A synthase from the crotonase fold superfamily. *PLoS One* 8, e63095.

(50) Morris, C. M., George, A., Wilson, W. W., and Champlin, F. R. (1995) Effect of polymyxin B nonapeptide on daptomycin permeability and cell surface properties in *Pseudomonas aeruginosa*, *Escherichia coli*, and *Pasteurella multocida*. *J. Antibiot.* 48, 67–72.

(51) Vaara, M. (1992) Agents that increase the permeability of the outer membrane. *Microbiol. Rev.* 56, 395–411.

(52) Collins, M. D., and Jones, D. (1981) Distribution of isoprenoid quinone structural types in bacteria and their taxonomic implication. *Microbiol. Rev.* 45, 316–354.

(53) Jeffries, L., Cawthorne, M. A., Harris, M., Diplock, A. T., Green, J., and Price, S. A. (1967) Distribution of menaquinones in aerobic Micrococaceae. *Nature* 215, 257–259.

(54) Paternotte, I., Fan, H. J., Screve, P., Claesen, M., Tulkens, P. M., and Sonveaux, E. (2001) Syntheses and hydrolysis of basic and dibasic ampicillin esters tailored for intracellular accumulation. *Bioorg. Med. Chem.* 9, 493–502.

(55) Moreira, R., Calheiros, T., Cabrita, J., Mendes, E., Pimentel, M., and Iley, J. (1996) Acyloxymethyl as a drug protecting group. Part 3. Tertiary O-amidomethyl esters of penicillin G: chemical hydrolysis and anti-bacterial activity. *Pharm. Res.* 13, 70–75.

(56) Lu, X., Zhou, R., Sharma, I., Li, X., Kumar, G., Swaminathan, S., Tonge, P. J., and Tan, D. S. (2012) Stable analogues of OSB-AMP: potent inhibitors of MenE, the *o*-succinylbenzoate-CoA synthetase from bacterial menaquinone biosynthesis. *ChemBioChem* 13, 129–136.

(57) Wiegand, I., Hilpert, K., and Hancock, R. E. (2008) Agar and broth dilution methods to determine the minimal inhibitory concentration (MIC) of antimicrobial substances. *Nat. Protoc.* 3, 163–175.

(58) Akinleye, A., Chen, Y., Mukhi, N., Song, Y., and Liu, D. (2013) Ibrutinib and novel BTK inhibitors in clinical development. *J. Hematol. Oncol.* 6, 59.

(59) Honigberg, L. A., Smith, A. M., Sirisawad, M., Verner, E., Loury, D., Chang, B., Li, S., Pan, Z., Thamm, D. H., Miller, R. A., and Buggy, J. J. (2010) The Bruton tyrosine kinase inhibitor PCI-32765 blocks B-cell activation and is efficacious in models of autoimmune disease and B-cell malignancy. *Proc. Natl. Acad. Sci. U. S. A.* 107, 13075–13080.

(60) Evans, E. K., Tester, R., Aslanian, S., Karp, R., Sheets, M., Labenski, M. T., Witowski, S. R., Lounsbury, H., Chaturvedi, P., Mazdiyasi, H., Zhu, Z., Nacht, M., Freed, M. I., Petter, R. C., Dubrovskiy, A., Singh, J., and Westlin, W. F. (2013) Inhibition of Btk with CC-292 provides early pharmacodynamic assessment of activity in mice and humans. *J. Pharmacol. Exp. Ther.* *346*, 219–228.

(61) Serafimova, I. M., Pufall, M. A., Krishnan, S., Duda, K., Cohen, M. S., Maglathlin, R. L., McFarland, J. M., Miller, R. M., Frodin, M., and Taunton, J. (2012) Reversible targeting of noncatalytic cysteines with chemically tuned electrophiles. *Nat. Chem. Biol.* *8*, 471–476.

(62) Bradshaw, J. M., McFarland, J. M., Paavilainen, V. O., Bisconte, A., Tam, D., Phan, V. T., Romanov, S., Finkle, D., Shu, J., Patel, V., Ton, T., Li, X., Loughhead, D. G., Nunn, P. A., Karr, D. E., Gerritsen, M. E., Funk, J. O., Owens, T. D., Verner, E., Brameld, K. A., Hill, R. J., Goldstein, D. M., and Taunton, J. (2015) Prolonged and tunable residence time using reversible covalent kinase inhibitors. *Nat. Chem. Biol.* *11*, 525–531.

(63) White, D. C., and Frerman, F. E. (1967) Extraction, characterization, and cellular localization of the lipids of *Staphylococcus aureus*. *J. Bacteriol.* *94*, 1854–1867.

(64) Onorato, J. M., Chen, L., Shipkova, P., Ma, Z., Azzara, A. V., Devenny, J. J., Liang, N., Haque, T. S., and Cheng, D. (2010) Liquid-liquid extraction coupled with LC/MS/MS for monitoring of malonyl-CoA in rat brain tissue. *Anal. Bioanal. Chem.* *397*, 3137–3142.

(65) Keshishian, H., Addona, T., Burgess, M., Kuhn, E., and Carr, S. A. (2007) Quantitative, multiplexed assays for low abundance proteins in plasma by targeted mass spectrometry and stable isotope dilution. *Mol. Cell. Proteomics* *6*, 2212–2229.

(66) Addona, T. A., Abbatiello, S. E., Schilling, B., Skates, S. J., Mani, D. R., Bunk, D. M., Spiegelman, C. H., Zimmerman, L. J., Ham, A. J., Keshishian, H., Hall, S. C., Allen, S., Blackman, R. K., Borchers, C. H., Buck, C., Cardasis, H. L., Cusack, M. P., Dodder, N. G., Gibson, B. W., Held, J. M., Hiltke, T., Jackson, A., Johansen, E. B., Kinsinger, C. R., Li, J., Mesri, M., Neubert, T. A., Niles, R. K., Pulsipher, T. C., Ransohoff, D., Rodriguez, H., Rudnick, P. A., Smith, D., Tabb, D. L., Tegeler, T. J., Variyath, A. M., Vega-Montoto, L. J., Wahlander, A., Waldemarson, S., Wang, M., Whiteaker, J. R., Zhao, L., Anderson, N. L., Fisher, S. J., Liebler, D. C., Paulovich, A. G., Regnier, F. E., Tempst, P., and Carr, S. A. (2009) Multi-site assessment of the precision and reproducibility of multiple reaction monitoring-based measurements of proteins in plasma. *Nat. Biotechnol.* *27*, 633–641.

(67) Alexander, E. L., Gardete, S., Bar, H. Y., Wells, M. T., Tomasz, A., and Rhee, K. Y. (2014) Intermediate-type vancomycin resistance (VISA) in genetically-distinct *Staphylococcus aureus* isolates is linked to specific, reversible metabolic alterations. *PLoS One* *9*, e97137.

(68) Nandakumar, M., Prosser, G. A., de Carvalho, L. P., and Rhee, K. (2015) Metabolomics of *Mycobacterium tuberculosis*. *Methods Mol. Biol.* *1285*, 105–115.

(69) Melter, O., and Radojevic, B. (2010) Small colony variants of *Staphylococcus aureus* – review. *Folia Microbiol. (Dordrecht, Neth.)* *55*, 548–558.

(70) Meganathan, R. (2001) Biosynthesis of menaquinone (vitamin K₂) and ubiquinone (coenzyme Q): a perspective on enzymatic mechanisms. *Vitam. Horm.* *61*, 173–218.

(71) Jiang, M., Chen, X., Guo, Z.-F., Cao, Y., Chen, M., and Guo, Z. (2008) Identification and characterization of (1R,6R)-2-succinyl-6-hydroxy-2,4-cyclohexadiene-1-carboxylate synthase in the menaquinone biosynthesis of *Escherichia coli*. *Biochemistry* *47*, 3426–3434.

(72) Widhalm, J. R., van Oostende, C., Furt, F., and Basset, G. J. (2009) A dedicated thioesterase of the Hotdog-fold family is required for the biosynthesis of the naphthoquinone ring of vitamin K₁. *Proc. Natl. Acad. Sci. U. S. A.* *106*, 5599–5603.

(73) Chen, M., Ma, X., Chen, X., Jiang, M., Song, H., and Guo, Z. (2013) Identification of a hotdog fold thioesterase involved in the biosynthesis of menaquinone in *Escherichia coli*. *J. Bacteriol.* *195*, 2768–2775.

(74) Hiratsuka, T., Furihata, K., Ishikawa, J., Yamashita, H., Itoh, N., Seto, H., and Dairi, T. (2008) An alternative menaquinone biosynthetic pathway operating in microorganisms. *Science* *321*, 1670–1673.